PAPER • OPEN ACCESS

Effects of the cap layer on the properties of AlN barrier HEMT grown on 6-inch Si(111) substrate

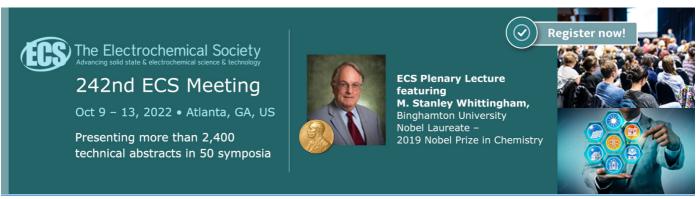To cite this article: Yuanyang Xia *et al* 2020 *Mater. Res. Express* **7** 065902

View the article online for updates and enhancements.

You may also like

Materials Research Express

PAPER

Effects of the cap layer on the properties of AlN barrier HEMT grown on 6-inch Si(111) substrate

Yuanyang Xia[1], Youhua Zhu[1,2,3] ⓘ, Chunhua Liu[1], Hongyuan Wei[1], Tingting Zhang[1], Yeeheng Lee[1], Tinggang Zhu[1], Meiyu wang[2], Li Yi[2] and Mei Ge[2]

1. CorEnergy Semiconductor Co., LTD, Zhangjiagang 215600, People's Republic of China
2. School of Information Science and Technology, Nantong University, Nantong 226019, People's Republic of China
3. Author to whom any correspondence should be addressed.

E-mail: ntyouhua@ntu.edu.cn

Abstract

A series of AlN/GaN heterostructures were grown on 150 mm Si substrates by metal organic chemical vapor deposition (MOCVD). Different cap layer structures, including gallium nitride (GaN) and silicon nitride (SiN_x), were used to passivate the heterostructure surface. A 3.5 nm thick SiN_x cap is able to maintain the two dimensional electron gas (2DEG) stability in a long period. An AlN/GaN heterostructure with a 4.5 nm thick AlN barrier exhibits the best 2DEG properties, in terms of sheet resistance, carrier mobility and stability. The carrier mobility of the 2DEG can be enhanced by a combination of SiNx and GaN cap layers to over 1400 cm^2/Vs.

1. Introduction

The commercialization of gallium nitride (GaN) based high electron mobility transistor (HEMT) has accelerated in recent years [1, 2], owing to its proven capability in reducing switching losses, sustaining high breakdown voltages, as well as maintaining high temperature stability [3]. The progress in the epitaxial growth of GaN on large size Si substrate reduces the production cost. Meanwhile, HEMT devices on Si can be easily integrated to the existing Si foundries [4–6]. The above benefits bring the GaN based HEMT device closer to the mass market applications.

The barrier layer is one of the key components in the HEMT device, which determines the resistance of the conduction channel. AlGaN is the most commonly used barrier material. The two-dimensional electron gas (2DEG) formed at the AlGaN/GaN interface region shows good stability, low sheet resistance, high carrier density, and high electron mobility [7, 8]. AlN as a barrier material also attracts attention due to the formation of even higher 2DEG density at the AlN/GaN interface region [9]. A sheet resistance (Rs) value as low as 128 Ω/sq has been reported, with a 2DEG density of 3.21 $\times$ 10^{13}/cm^2 [10]. Besides, the alloy scattering can be avoided in the AlN system, which enhances the 2DEG hall mobility [11, 12]. AlN barrier based HEMT devices, with low gate leakage and high I_{on}/I_{off} ratio, has been demonstrated [13]. Table 1. summarizes the recent studies on AlN/GaN heterostructures with the best Rs performances.

However, the relaxation of AlN is one major challenge, due to the large lattice mismatch (2.5%) with the GaN channel layer. Silicon nitride (SiN_x) cap has been employed as a surface passivation layer to avoid/reduce the AlN relaxation [14]. However, the effect of the composition and thickness of the passivation cap layer on suppressing the relaxation has rarely been studied. In this paper, we reported on the long term 2DEG stability of the AlN/GaN heterostructure incorporating *in situ* grown GaN and/or SiN_x cap layers.

2. Experiments

A series of AlN/GaN heterostructures were prepared in an Aixtron close coupled showerhead (CCS) 6 $\times$ 2 MOCVD system on 150 mm highly resistive ($>$3000 $\Omega \cdot$ cm) Si (111) wafers. Trimethylgallium (TMGa) and

Table 1. Summary of the AlN/GaN ultrathin heterostructure parameters.

Sample	AlN (nm)	Cap (nm)	Substrate	Rs (Ω/sq)	Ns (/cm^2)	Growth method
[14]	6	6 (SiN$_x$)	Si	186	2.5e13	MOCVD
[15]	4.5	1 (GaN)	sapphire	409	2.2e13	MBE
[10]	3.5	none	sapphire	128	3.2e13	MBE
[12]	3	2 (GaN)	sapphire		1.3e12	MOCVD
D	6	3.5 (SiN$_x$)	Si	178	3.9e13	MOCVD

Table 2. Structural parameters of samples A-H.

sample	AlN barrier thickness (nm)	GaN cap thickness (nm)	SiNx cap thickness (nm)
A	7	0	0
B	7	0	2
C	7	0	3.5
D	6	0	3.5
E	4.5	0	3.5
F	3.5	0	3.5
G	2.5	0	3.5
H	4.5	2	3.5

trimethylallunium (TMAl) were used to provide the metal elements, while ammonia (NH$_3$) was used as the group V precursor. The Si wafer was first heated to 1050 °C in hydrogen (H$_2$) to remove the native oxide before growth. After a short TMAl pretreatment, a 150 nm AlN nucleation layer was deposited. During the AlN growth, a very low V/III ratio ($\sim$30) was used to suppress the gas phase reactions of TMAl. After that, four layers of step graded AlGaN were grown, and the Al contents were 0.60, 0.50, 0.40 and 0.25, respectively. The total thickness of the AlGaN buffer layer was $\sim$1000 nm. Then, a 1000 nm thick unintentionally doped GaN channel layer was grown. H$_2$ was used as the carrier gas during the (Al, Ga) N buffer and the GaN channel layer growth. The AlN barrier layer with thicknesses ranging from 2.5 to 7 nm was grown at $\sim$900 °C. Nitrogen (N$_2$) was used as the carrier gas, which promotes the diffusion of Al atoms on the surface, and suppresses the GaN decomposition in a low NH$_3$ ambient. During the AlN barrier growth, trimethylindium (TMIn) was used as a surfactant to improve the layer quality. Unintentional gallium incorporation during the InAlN alloy growth in CCS reactors has been demonstrated [16–18]. It may also happen during the (In)AlN barrier growth and impact the 2DEG properties. Finally, the *in situ* SiN$_x$ cap layers with different thicknesses were deposited at the AlN barrier growth temperature, i.e., 900 °C. The NH$_3$/SiH$_4$ ratio during the growth was $\sim$3500, and the growth rate was $\sim$1.3 μm h^{-1} After cooling down, the bow of these wafers was measured to be less than 10 μm and the surface was crack free with <3 mm edge exclusion. Table 2 lists all the structural parameters of the samples studied.

A Lehighton contactless mobility mapping system (LEI-1600) was used to measure and map the sheet resistance of the heterostructure across the whole wafer. The 2DEG sheet carrier density and mobility can also be measured, using Hall method embedded in the LEI-1600 system [19]. The Park XE15 Atomic Force Microscope (AFM) was used to evaluate the sample surface roughness. The Bruker D8 Discover x-ray diffraction (XRD) tool was used to characterize the Al composition in the step-graded buffer layer. The AlN barrier and cap layer thicknesses were deduced from the x-ray reflectivity (XRR) curves, which were also measured by the Bruker D8 XRD system.

3. Results

To study the influence of SiN$_x$ cap layer thickness on the relaxation behavior of AlN barrier, *in situ* grown SiN$_x$ layer with thicknesses of 0 (no cap layer), 2.0 and 3.5 nm on the same AlN/GaN heterostructure were prepared, labeled as sample A, B and C, respectively. The AlN barrier thickness was 7 nm. Due to the large lattice mismatch, strong tensile stress exists in the AlN layers grown on GaN, and the critical thickness was reported in the range of 6–8 nm [20]. Therefore, the current heterostructure could possibly undergo a lattice relaxation after the epitaxial growth. The Rs values of these samples were recorded once per week in the following month. Figure 1 showed the sheet resistance changes of the AlN/GaN heterostructure as a function of time after growth. The initial R$_s$ values for samples A, B and C were 320, 192 and 190 Ω/sq, respectively. Among these samples, sample C exhibited the highest R$_s$ stability, with a $\sim$10% increase from 190 to 209 Ω/sq three weeks later.
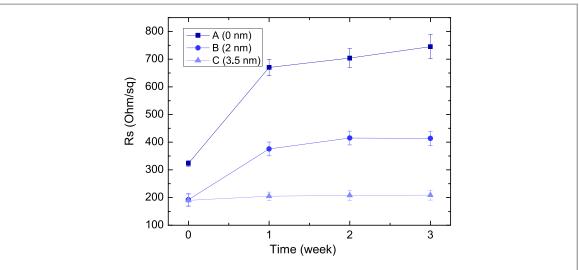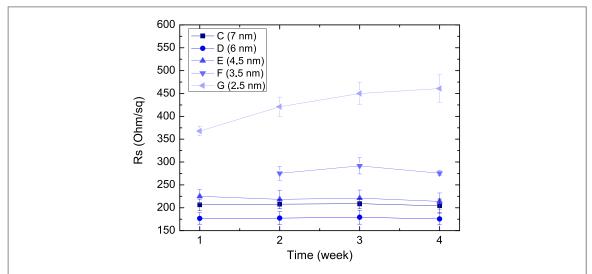
Figure 1. The variation of the R$_s$ of AlN/GaN heterostructures with SiN$_x$ cap layer thickness ranging from 0 to 3.5 nm. The AlN barrier thickness is 7 nm.
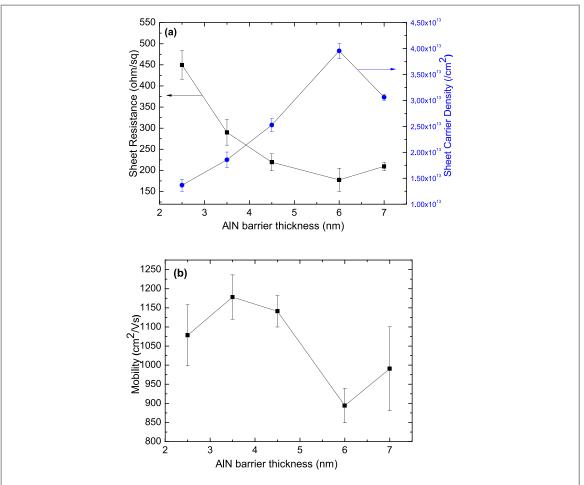

Figure 2. The variation of R$_s$ as a function of time, for AlN barrier thicknesses ranging from 2.5 to 7 nm. All the samples have a 3.5 nm thick SiN$_x$ cap layer.

Actually, the Rs value remained almost unchanged after the second week, which indicates a stable structure in sample C. In contrast, the R$_s$ of samples A and B quickly increased in the first week and gradually stabilized afterwards. The R$_s$ of sample A, which has no SiN$_x$ cap layer, deteriorated ~133% from 320 to 748 Ω/sq by the end of the third week. This change is mainly due to the sheet carrier density decrease, suggesting that a strong relaxation in the AlN layer happened. Based on the observed R$_s$ changes, the degrees of barrier layer relaxation depends on growth conditions, barrier thickness, as well as the cap layer design. The much higher initial R$_s$ value of sample A with a 7 nm AlN barrier could also imply a fast early stage relaxation right after growth completion. The oxidation of AlN may also contribute to the Rs increase, as the AlN barrier is exposed directly to the atmosphere environment, without the protection of a cap layer.

Next, we investigated the Rs stability with different AlN barrier thicknesses, ranging from 2.5 to 7 nm, as shown in table 1. These samples all had a 3.5 nm SiN$_x$ cap layer, which was effective in improving the R$_s$ stability of the AlN/GaN heterostructures. The time evolution of R$_s$ was recorded over a month, as illustrated in figure 2. All samples with AlN barrier thicker than 3 nm showed stable R$_s$ values during this timeframe. The only sizable increase in the R$_s$ was observed from sample G, which has a barrier thickness of 2.5 nm. The root cause of this increase is still under investigation.

Figure 3(a) showed the variation of R$_s$ and carrier density (N$_s$) as a function of the barrier layer thickness. Data were collected three weeks after growth, when the electrical and structural parameters of the heterostructures became stable. When the AlN barrier was thinner than 6 nm, the Rs value decreased from 452 to 178 Ω/sq with the increasing barrier thickness. The Rs increased slightly to 209 Ω/sq when the barrier was
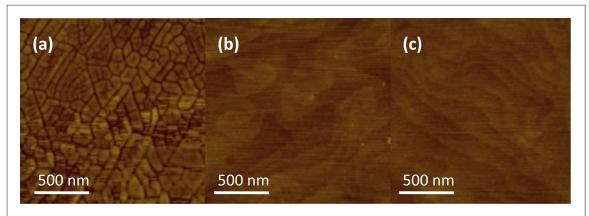
Figure 3. The variation of (a) R_s and N_s, (b) carrier mobility as a function of the AlN barrier thickness. All the samples have a SiN_x cap layer thickness of 3.5 nm.

7 nm. The R_s variation was closely correlated with that of carrier sheet density (N_s), as also shown in figure 3(a). When the barrier was relatively thin, the accumulation of 2DEG increased as the AlN thickness increased, reducing the sheet resistance. When the barrier thickness increased to 7 nm, a decrease of N_s was observed. It could be attributed to the relaxation of AlN layer, as it approaches the critical thickness of AlN on GaN [20]. Carrier mobility was another important 2DEG parameter. A higher mobility translated to a higher transconductance of the HEMT devices [21–23]. Figure 3(b) showed the carrier mobility as a function of the barrier thickness. The highest mobility of 1178 cm^2/Vs was observed when the barrier was 3.5 nm. It dropped to a low value of 893 cm^2/Vs when the barrier was 6 nm concomitant with the highest carrier density. The degraded mobility could be attributed to the stronger interfacial scattering when the peak of 2DEG was shifted closer to the AlN/GaN interface [15]. Finally, the decrease of N_s and mobility leads to the increase of R_s, when the AlN barrier is thick (>6 nm).

Figure 4(a) showed the surface morphology of sample A, which has a 7 nm thick AlN barrier and no cap layer was grown. The measurements were conducted one month after growth. Lot of cracks presented on the surface, which should be the result of lattice relaxation. It gave an explanation to the significant Rs increase observed in figure 1. Figure 4(b) showed the surface of sample C, which has a 7 nm thick barrier and 3.5 nm thick SiNx cap layer. The surface is still very smooth over one month after growth, with a root mean square (RMS) roughness as low as 0.20 nm. The stable surface state is one important reason for the stable Rs performance. The comparison between the surface state of sample A and C suggested that a SiNx cap may counter balance the tensile strain in the AlN barrier, and maintain a stable surface state. Similar surface characteristics have been observed by Cheng *et al* in [14]. The above results indicate that a SiNx cap is effective in improving the reliability of AlN barrier HEMT devices.

In order to fabricate a high performance HEMT device, both low 2DEG sheet resistance and high electron mobility are desired. Although the 4.5 nm AlN barrier gave a slightly lower carrier mobility than that of 3.5 nm barrier, the Rs value was much lower. Therefore, we used the 4.5 nm AlN barrier as a baseline to further improve the mobility. In sample H, a 2 nm thick GaN cap layer was inserted between the 4.5 nm AlN barrier and the 3.5 nm SiN_x cap. As shown in figure 4(c), a smooth surface with RMS roughness of ~0.19 nm was obtained. No

Figure 4. Surface morphology of sample A(a), C(b) and H(c), characterized by the tapping mode AFM. The scan scales are all $2 \times 2\ \mu m^2$ and the RMS roughness are 0.40, 0.20 and 0.19 respectively. The z-scale is 5 nm.
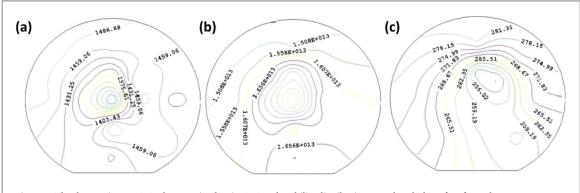

Figure 5. The sheet resistance (R_s), sheet carrier density (N_s) and mobility distribution over the whole wafer of sample H.

sign of relaxation was observed. Figure 5 showed the sheet resistance, sheet carrier density and mobility mapping of sample H. The average carrier mobility is enhanced to 1423 cm^2/Vs, which is among the highest values reported for the same AlN/GaN HEMT devices on Si substrates by MOCVD [14, 15]. Compared to sample E, the mobility was enhanced by ~29%, even though the carrier density dropped from 2.66 $\times$ 10^{13} to 1.70 $\times$ 10^{13}/cm^3. As GaN has a smaller bandgap than AlN, the insertion of GaN modified the conduction band edge relative to the Fermi level, thus partially depletes the carriers in the 2DEG channel [24]. According to previous discussions, the enhancement of the mobility could be partially attributed to the reduced interfacial carrier scattering. The sheet resistance, which was a product of carrier density and mobility, increased from 225 to 259 Ω/sq. This value was still among the best reported in the literature. As shown in figure 3(a), the sheet resistances are very sensitive to the AlN barrier thicknesses, which could be further related to the growth temperature. By carefully adjusting the wafer temperature distribution during the growth, an AlN thickness uniformity of 1% was obtained, and it resulted in a high Rs uniformity of ~3%, as illustrated in figure 5(c). The 2DEG properties were examined again after one month and no appreciable changes of R$_s$, N$_s$ and mobility were observed. We believe that both SiN$_x$ and GaN cap layers contribute to the long term stability of the AlN/GaN heterostructure. Further enhancement of the 2DEG mobility could be achieved by optimizing the growth conditions [10].

4. Conclusions

AlN/GaN heterostructures with different AlN barrier thicknesses and cap layers were studied. The cap layer structure has significant effects on the initial 2DEG properties, as well as the long term stability. SiN$_x$ cap was proven to be able to suppress the AlN relaxation. It was found that a 3.5 nm SiN$_x$ cap could adequately maintain the 2DEG stability after a long period of storage time. A 4.5 nm barrier AlN/GaN HEMT device with 3.5 nm SiN$_x$ cap layer showed good performance and stability in terms of sheet resistance, carrier density and mobility. We further demonstrated that an additional GaN cap layer could improve the 2DEG mobility.

Acknowledgments

ORCID iDs

Youhua Zhu ⬤ https://orcid.org/0000-0002-9004-3121

References

[1] Roberts J, Lafontaine H and McKnight-Macneil C 2014 Advanced SPICE models applied to high power GaN devices and integrated GaN drive circuits *IEEE Applied Power Electronics Conf. and Exposition (Fort Worth, TX)* 493

[2] Parikh P *et al* 2014 Commercialization of 600 V GaN HEMTs *SSDM (Tsukuba)* (https://doi.org/10.7567/SSDM.2014.E-3-1)

[3] Lidow A, Strydom J, de Rooij M and Reusch D 2014 *GaN Transistors for Efficiency Power Conversion* 2nd edn (El Segundo, CA: Wiley)

[4] Lee K T *et al* 2017 GaN devices on a 200 mm Si platform targeting heterogeneous integration *IEEE Electron Device Lett.* **38** 1094–6

[5] Marcon D, Jaeger B D, Halder S, Vranckx N, Mannaert G, Hove M V and Decoutere S 2013 Manufacturing challenges of GaN-on-Si HEMTs in a 200 mm CMOS Fab *IEEE Trans. Semicond. Manuf.* **26** 361–7

[6] Hoke W E *et al* 2012 Monolithic integration of silicon CMOS and GaN transistors in a current mirror circuit *Journal of Vacuum Science & Technology B, Nanotechnology and Microelectronics: Materials, Processing, Measurement, and Phenomena* **30** 02B101

[7] Hoke W E, Kennedy T D, Torabi A, Lyman P S, Howsare C A and Schultz B D 2014 Highly uniform AlGaN/GaN HEMT films grown on 200-mm silicon substrates by plasma molecular beam epitaxy *Journal of Vacuum Science & Technology B, Nanotechnology and Microelectronics: Materials, Processing, Measurement, and Phenomena* **32** 030605

[8] Sury C, Curutchet A, Malbert N and Labat N 2009 Low frequency noise evolution of AlGaN/GaN HEMT after 2000 h of HTRB and HTO life tests *AIP Conf. Proc.* **1129** 625

[9] Ambacher O *et al* 2000 Two dimensional electron gases induced by spontaneous and piezoelectric polarization in undoped and doped AlGaN/GaN heterostructures *J. Appl. Phys.* **87** 334–44

[10] Cao Y, Wang K, Li G, Kosel T, Xing H and Jena D 2011 MBE growth of high conductivity single and multiple AlN/GaN heterojunctions *J. Cryst. Growth* **323** 529–33

[11] Xie X, Gao K, Li S, Zhou D, Zhou W, Sun Y and Lin T 2019 Magneto-transport property of an AlInN/AlN/GaN heterostructure *Physica B* **562** 112–5

[12] Narin P, Arslan E, Ozturk M, Ozturk M, Lisesivdin S B and Ozbay E 2019 Scattering analysis of ultrathin barrier (<7 nm) GaN-based heterostructures *Appl. Phys. A* **125** 278

[13] Baca A, Armstrong A, Allerman A, Douglas E, Sanchez C, King M, Coltrin M, Fortune T and Kaplar R 2016 An AlN/Al0.85Ga0.15N high electron mobility transistor *Appl. Phys. Lett.* **109** 033509

[14] Cheng K, Degroote S, Leys M, Medjdoub F, Derluyn J, Sijmus B, Germain M and Borghs G 2011 AlN/GaN heterostructures grown by metal organic vapor phase epitaxy with *in situ* Si₃N₄ passivation *J. Cryst. Growth* **315** 204–7

[15] Bairamis A, Zervos C, Adikimenakis A, Kostopoulos A, Kayambaki M, Tsagaraki K, Konstantinidis G and Georgakilas A 2014 Electron density and currents of AlN/GaN high electron mobility transistors with thin GaN/AlN buffer layer *Appl. Phys. Lett.* **105** 113508

[16] Hiroki M, Oda Y, Watanabe N, Maeda N, Yokoyama H, Kumakura K and Yamamoto H 2013 Unintensional Ga incorporation in metalorganic vapor phase epitaxy of In-containing III-nitride semiconductors *J. Crystal Growth* **382** 36–40

[17] Bouveyron R and Charles M 2017 Growth by MOCVD of In(Ga)AlN alloys, and a study of gallium contamination in these layers under nitrogen and hydrogen carrier gas *J. Crystal Growth* **464** 105–11

[18] Zhou K, Ren H, Ikeda M, Liu J, Ma Y, Gao S, Tang C, Li D, Zhang L and Yang H 2017 Unintentional gallium incorporation in InGaN layers during epitaxial growth *Superlattices Microstruct.* **101** 323–8

[19] LEI-1600 series mobility measurement system theory of operation https://semilab.com/category/products/non-contact-sheet-resistance-by-eddy-current

[20] Cao Y and Jena D 2007 High-mobility window for two-dimensional electron gases at ultrathin AlN/GaN heterojunctions *Appl. Phys. Lett.* **90** 182112

[21] Alekseev E, Eisenbach A and Pavlidis D 1999 Low interface state density AlN/GaN MISFETs *Electron. Lett* **35** 2145–6

[22] Higashiwaki M, Mimura T and Matsui T 2006 AlN/GaN insulated-gate HFETs using cat-CVD SiN *IEEE Electron Device Lett.* **27** 719–21

[23] Kawai H, Hara M, Nakamura F and Imanaga S 1998 AlN/GaN insulated gate heterostructure FET with regrown n + GaN ohmic contact *Electron. Lett* **34** 592–3 AlN/GaN insulated gate heterostructure FET with regrown n+GaN ohmic contactAlN/GaN insulated gate heterostructure FET with regrown n+GaN ohmic contact

[24] Mizutani T, Yamada H, Kishimoto S and Nakamura F 2013 Normally off AlGaN/GaN high electron mobility transistors with p-InGaN cap layer *J. Appl. Phys.* **113** 034502